Cellular/Molecular

Transsynaptic Assemblies Link Domains of Presynaptic and Postsynaptic Intracellular Structures across the Synaptic Cleft

Andy A. Cole and Thomas S. Reese
Laboratory of Neurobiology, National Institute of Neurological Disorders and Stroke, National Institutes of Health, Bethesda, Maryland 20892

The chemical synapse is a complex machine separated into three parts: presynaptic, postsynaptic, and cleft. Super-resolution light microscopy has revealed alignment of presynaptic vesicle release machinery and postsynaptic neurotransmitter-receptors and scaffolding components in synapse spanning nanocolumns. Cryo-electron tomography confirmed that postsynaptic glutamate receptor-like structures align with presynaptic structures in proximity to synaptic vesicles into transsynaptic assemblies. In our electron tomographic renderings, nearly all transcleft structures visibly connect to intracellular structures through transmembrane structures to form transsynaptic assemblies, potentially providing a structural basis for transsynaptic alignment. Here, we describe the patterns of composition, distribution, and interactions of all assemblies spanning the synapse by producing three-dimensional renderings of all visibly connected structures in excitatory and inhibitory synapses in dissociated rat hippocampal neuronal cultures of both sexes prepared by high-pressure freezing and freeze-substitution. The majority of transcleft structures connect to material in both presynaptic and postsynaptic compartments. We found several instances of assemblies connecting to both synaptic vesicles and postsynaptic density scaffolding. Each excitatory synaptic vesicle within 30 nm of the active zone contacts one or more assembly. Further, intracellular structures were often shared between assemblies, entangling them to form larger complexes or association domains, often in small clusters of vesicles. Our findings suggest that transsynaptic assemblies physically connect the three compartments, allow for coordinated molecular organization, and may combine to form specialized functional association domains, resembling the light-level nanocolumns.

Key words: **cell adhesion; chemical synapse; electron tomography; nanocolumn; nanodomain; transsynaptic assembly**

Significance Statement

A recent tomographic study uncovered that receptor-like cleft structures align across the synapse. These aligned structures were designated as transsynaptic assemblies and demonstrate the coordinated organization of synaptic transmission molecules between compartments. Our present tomographic study expands on the definition of transsynaptic assemblies by analyzing the three-dimensional distribution and connectivity of all cleft-spanning structures and their connected intracellular structures. While one-to-one component alignment occurs across the synapse, we find that many assemblies share components, leading to a complex entanglement of assemblies, typically around clusters of synaptic vesicles. Transsynaptic assemblies appear to form domains which may be the structural basis for alignment of molecular nanodomains into synapse spanning nanocolumns described by super-resolution light microscopy.

Introduction

Analyzing detailed synaptic structure and organization with electron tomography has expanded our understanding of the synapse. Electron tomography revealed the complex three-dimensional (3D) scaffolding system of vertically and horizontally oriented molecular structures that provide stability for the array of postsynaptic receptors in the postsynaptic density (Chen et al., 2008a, 2015). Further, tomography was used to demonstrate that the inhibitory postsynaptic compartment is instead a loose, vertically oriented system filled with small interlinking molecules, thought to be a gephyrin network (Linsalata et al., 2014). In the presynaptic compartment, tomography revealed small filaments linking synaptic vesicles to the active zone membrane, another filament type

Received Nov. 28, 2022; revised June 6, 2023; accepted June 8, 2023.

Author contributions: T.S.R. and A.A.C. designed research; A.A.C. performed research; T.S.R. and A.A.C. analyzed data; T.S.R. and A.A.C. edited the paper; A.A.C. wrote the first draft of the paper; A.A.C. wrote the paper.

This research was supported by the Division of Intramural Research of the National Institutes of Health (NIH), National Institute of Neurological Disorders and Stroke Grant NS002972-25. We thank Dr. Richard Leapman, National Institute of Biomedical Imaging and Bioengineering, NIH, for the use of his FEI Tecnai 300 kV electron microscope and his support in the acquisition of tomographic data; Dr. Xiaobing Chen and Dr. Alexander Linsalata for acquiring and processing tomographic data; Rita Azzam and Virginia Crocker for preparing the sections for tomography; and Christine Winters for preparing hippocampal cultures as well as performing high-pressure freezing and freeze-substitution for tomography.

The authors declare no competing financial interests.

Correspondence should be addressed to Andy A. Cole at cole.andy.a@gmail.com.

https://doi.org/10.1523/JNEUROSCI.2195-22.2023

connecting vesicles together into a cohesive vesicle cloud (Landis et al., 1988; Hirokawa et al., 1989; Siksou et al., 2009; Fernández-Busnadiego et al., 2010; Burette et al., 2012; Szule et al., 2012; Watanabe et al., 2013; Cole et al., 2016), and a final, longer filament type connecting vesicles in a skein to form a pathway through the vesicle cloud to the active zone membrane (Cole et al., 2016). In the cleft, tomography revealed transcleft filaments of several different types bridging the synapse, with each type possessing different distribution patterns (Burette et al., 2012; High et al., 2015). Each compartment has largely been considered independent of the others' influence. However, recent discoveries indicate that synaptic molecules align across the cleft, and thus, compartments are influencing each other. For example, super-resolution light microscopy demonstrated transsynaptic dynamic alignment of presynaptic Rim1/2 proteins with postsynaptic PSD-95 proteins (Tang et al., 2016), while a subsequent electron tomography study discovered *transsynaptic assemblies*: postsynaptic structures, some resembling AMPA receptors, aligning or connecting to presynaptic structures near synaptic vesicles (Martinez-Sanchez et al., 2021). It appears that a complete understanding of the organizational principles of any one synaptic compartment requires a detailed three-dimensional description of how that compartment interacts or aligns with the others. While there are other possible mechanisms underlying molecular alignment across compartments, studies of synaptic cell adhesion molecule interactions (Missler et al., 2012; Südhof, 2017) and the transsynaptic assemblies in Martinez-Sanchez et al. (2021) support a physical mechanism, which we will explore with electron tomography.

Synaptic cell adhesion molecules provide a physical link across the cleft and into the cell, as a plethora of synaptic adhesion complexes interact with intracellular proteins, including presynaptic vesicle release machinery and postsynaptic receptors (Südhof, 2017). High et al. (2015) mapped the distribution of transcleft filaments and interpreted them as synaptic cell adhesion molecules paired across the cleft. We build on that work by examining the structure and distribution of all structures visibly connected to transcleft filaments in dissociated rat hippocampal neuron cultures that were high-pressure frozen, freeze substituted, imaged by electron tomography, and then segmented by hand and threshold methods. This provides detailed information about the structure and distribution of the entire menagerie of synaptic proteins.

Transsynaptic assemblies were defined as aligned or linked presynaptic and postsynaptic structures (Martinez-Sanchez et al., 2021). However, our renderings reveal that transcleft filaments can connect to multiple intracellular structures. These structures can be shared between assemblies, and as they are connected by shared structures, some associated assemblies could be forming larger functional alignment domains across the synapse. This suggests that transsynaptic assemblies can form both one-to-one alignment of individual structures across the synapse, as previously shown, and the more complex shared assemblies that form association domains. The association domain appears similar in size and location to the nanocolumns described in light-level studies by Tang et al. (2016). This descriptive study expands on the definition of transsynaptic assemblies and provides insights into their complex organization.

Materials and Methods

Cultures

Dissociated rat hippocampal neuron cultures were cultured directly in Bal-Tec gold specimen chambers, 3 mm wide and 300 μm deep. The neurons were prepared by papain dissociation from E19 rat fetuses of both sexes and plated on a confluent hippocampal glial layer that had been previously grown in the specimen chambers. Cultures were incubated at 10% CO_2 at 35°C in a medium of modified MEM with 6 g/l glucose (320–330 Osm), 2 mM Glutamax 1, 2% fetal bovine serum, 5% horse serum, and N3 (a growth factor cocktail of apotransferrin, putrescine, selenium, triiodothyronine, insulin, progesterone, and corticosterone; Mayer and Vyklicky, 1989; Chen et al., 2011) for three weeks.

High-pressure freezing and freeze substitution

In preparation, the culture media was exchanged for a solution of 124 mM NaCl, 2 mM KCl, 1.24 mM KH_2PO_4, 1.3 mM $MgCl_2$, 2.5 mM $CaCl_2$, 30 mM glucose, 25 mM HEPES, and 0.5% ovalbumin, pH 7.4 (325 Osm). Immediately before freezing, 1-hexadecene was layered directly over the medium in the gold chamber to prevent air pockets, and a second gold specimen chamber was placed on top of the first to form an enclosed chamber and fit the specimen chamber holder.

For freeze substitution, a layer of 4% acrolein in HPLC-grade acetone was frozen on top of frozen saturated uranyl acetate in a scintillation vial at −160°C. Under liquid nitrogen, frozen samples were place on top of the frozen solutions and capped. Samples were then placed in an AFS Unit (Leica Microsystems) programmed to execute the following schedule: hold at −160°C for 15 min; rise from −160 to −90°C over 14 h; hold at −90°C for 8 h; rise from −90 to −60°C over 6 h; and hold at −60°C for 12 h (Chen et al., 2008a). The specimens were thoroughly rinsed with chilled acetone and infiltrated with graded Lowicryl concentrations made with HPLC grade acetone 50%, 70%, and 100% during the day and 100% overnight. Specimens were put in histochemistry molds with freshly prepared 100% Lowicryl HM20 resin in acetone and polymerized by UV at −50°C, in the AFS Unit over 2 d. Last, the temperature was raised to 20°C over 70 h (Chen et al., 2014).

En face sections were cut between 100 and 200 nm thick and mounted on carbon-coated formvar grids. Ten-nanometer fiducial markers were added to both sides of the grid for calculating the tomographic reconstructions (Chen et al., 2008b).

Electron tomography

Synapse types were differentiated before tomographic imaging. Asymmetric synapses with large vesicles clusters and dense postsynaptic density were classified as excitatory synapses (Chen et al., 2008a,b, 2011). Symmetric synapses with a large vesicle cloud without a dense postsynaptic density were classified as inhibitory (Gray, 1969; Linsalata et al., 2014).

The synapses of interest were imaged using an FEI Tecnai 300-kV electron microscope with field-emission gun at 300-kV accelerating voltage. Each synapse was imaged from 74° to −74° tilt with 2° increments, rotated 90°, and imaged again. The two image-series were reconstructed separately then combined using IMOD (University of Colorado; Kremer et al., 1996). IMOD estimated the pixel size to be between 0.48 and 0.75 nm in 2048 × 2048, but images were binned such that the final pixel size was estimated between 1 and 1.4 nm in the final 3D volume. The resulting 3D volume tomograms were analyzed and segmented using Amira (Thermo Fisher Scientific). In Amira, pixel size was set at the upper range of 1.4 nm with voxels of 2.74 nm^3. All three compartments of the synapse had comparable quality and preservation of structure to be included in analysis. Three excitatory and two inhibitory tomograms were fully analyzed. Some of these tomograms have been partially analyzed for other publications (Chen et al., 2008a; Linsalata et al., 2014; High et al., 2015; Cole et al., 2016); however, segmentation data, renderings, and analysis are unique.

Segmentation

All segmentation was done using Amira software. Each tomogram was first segmented by local thresholding and then by hand. Segmentation began with identifying an electron-dense structure that spans the cleft. That structure and all connected transmembrane and intracellular structures were segmented. Other than synaptic membrane and synaptic vesicles (segmented by hand), no structures were included in any renderings or analysis that could not be traced back to a transcleft electron-

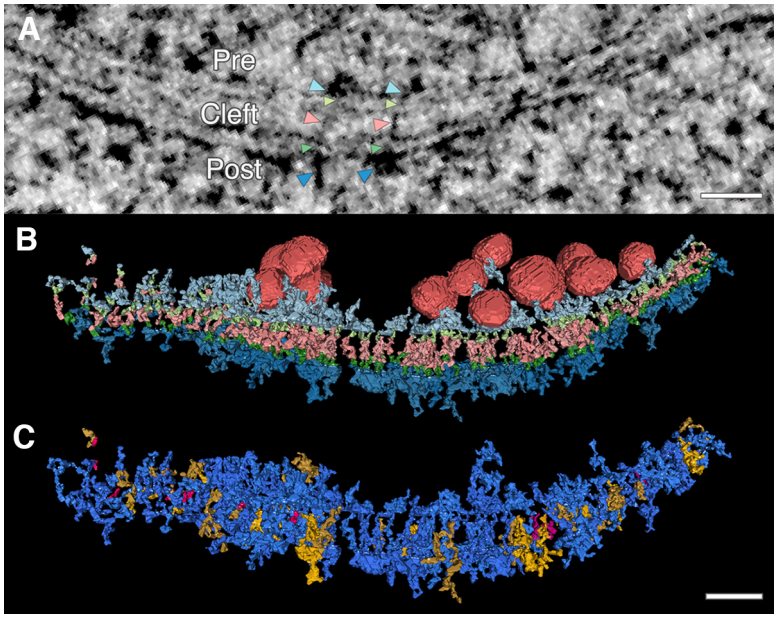

Figure 1. Electron tomography reveals extensive transsynaptic connection of intracellular structures throughout the synapse. Transcleft, transmembrane, and intracellular electron-dense structures were hand segmented and rendered in 3D from electron tomograms of high-pressure frozen and freeze-substituted mature dissociated rat hippocampal neuronal cultures. ***A***, | Transsynaptic assemblies, or assemblies of connected electron-dense material (black pixels) that span the synapse, are found in 15-nm virtual projections, as seen here. Color coded arrowheads indicate structures of two transsynaptic assemblies. Light blue arrowheads point to presynaptic (pre) membrane-bound structures. Light green arrowheads point to presynaptic transmembrane structures. Pink arrowheads point to transcleft (cleft) structures. Dark green arrowheads point to postsynaptic transmembrane structures. Dark blue arrowheads point to postsynaptic (post) membrane-bound structures. ***B***, A single synapse is rendered with synaptic vesicles (red) associated with transsynaptic assembly and all assembly structures (color coded the same as arrowheads in ***A*** to indicate the abundance of structures on both sides of the synapse connecting to transcleft structures. ***C***, Transsynaptic assemblies further classified with a different color code. An assembly with no intracellular structure is considered transcleft only (pink); an assembly that contains a transcleft structure connect to an intracellular structure on one side of the synapse is classified as a partial assembly (yellow); and an assembly with a transcleft structure connected to intracellular structures on both sides is classified as full transsynaptic assembly (blue). Scale bars: 40 nm.

dense structure. For membranous objects like vesicles and membrane, the nonelectron-dense area between membrane leaflets was segmented in three orthogonal planes to produce continuous spheres or sheets.

For hand segmentation, structures were identified and segmented in three orthogonal planes, leading to complete and interpretable renderings. Transcleft structures must have spanned the cleft completely. Transmembrane structures had to touch a transcleft structure and span the inner and outer plasma-membrane leaflets. Intracellular structures had to touch a transmembrane structure. Additionally, the lateral and vertical dimensions of intracellular structures were cutoff at ~70 nm, to limit sprawling structures caused by membrane staining artifacts. The segmentation of an object ended when it became discontinuous, when the morphology drastically changed, or it abutted a membrane boundary.

Because thresholding an entire virtual slice or tomogram led to massive and uninformative structures, a local thresholding method was used. A 3D region of interest was made around objects of interest with an approximately six-pixel buffer from the edge of the structure on all sides not bounded by membrane edges, in each virtual section. Using Amira software's wand tool, a local threshold was seeded within the electron-dense region of the object of interest. Masking and contrast-threshold values were set such that the renderings depicted the electron-dense structure in all three planes. Unfortunately, saturated black levels produced artifactitious discontinuities in some structures. Because we find hand segmentation provides more precise morphology, most data reported are from hand segmented sets except when reporting inhibitory data.

For inhibitory datasets, local thresholding segmentation was applied completely as above; however, only transsynaptic assemblies with synaptic vesicle association were hand segmented to compare against similar vesicle-associated assemblies in excitatory hand segmentation. Comparisons across excitatory and inhibitory datasets were done with thresholding data.

Rendering and measurements

The surface-rendering algorithms trim and smooth segmentation, which can make small objects appear smaller and discontinuous. Here, we used Amira's surface-rendering algorithm to produce surface models without additional smoothing. Volume and center-point data for each object was generated using Amira's Material Statistics module.

The synaptic center-point for each dataset was estimated such that it was mid-cleft, midway between left and rightmost synaptic vesicles near the active zone membrane, and midway through the usable *z*-axis of the dataset. The center-point for transsynaptic assemblies is set as the volumetric center-point of its transcleft structure.

Renderings were visualized using RStudio with the Tidyverse (Wickham et al., 2019), Natverse (Bates et al., 2020), and rgl (Murdoch and Adler, 2022) R packages.

Results

Transcleft filaments tether intracellular components into synapse spanning assemblies

Tomographs were made from mature synapses of rat dissociated hippocampal cell cultures. Excitatory and inhibitory synapses were differentiated based on their characteristic structures before imaging and segmentation (Gray, 1969; Chen et al., 2008a; Linsalata et al., 2014). Segmentation focused on membrane-bound intracellular material that connected to cleft-spanning or *transcleft* structures through transmembrane structures (Fig. 1).

In segmented clefts, 89% (242 of 267) of transcleft structures connected to membrane-bound intracellular structures. 65% (173 of 267) connected to structures in both presynaptic and postsynaptic compartments (Fig. 1*C*). Transcleft structures were observed to connect with up to four presynaptic or six postsynaptic intracellular structures. However, because

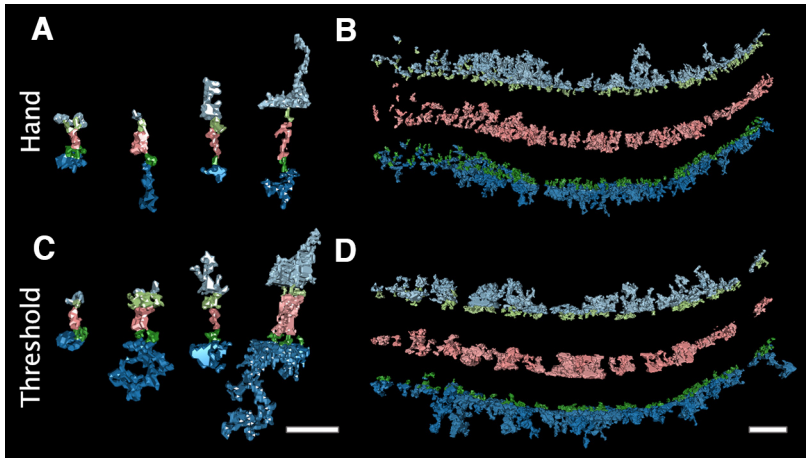

Figure 2. Both hand and local thresholding segmentation methods yield transsynaptic assemblies connected by transmembrane structures. Local thresholding was used as an alternative segmenting method. For this method, thresholds were applied to small 3D regions of interests around electron-dense structures. To be included in renderings, an intracellular structure must contact a transmembrane and cleft structure. ***A***, Examples of hand segmented transcleft structures (pink) from each excitatory synapse are shown with connecting presynaptic transmembrane and intracellular membrane-bound structures (light green and light blue, respectively), postsynaptic transmembrane and intracellular structures (dark green and blue, respectively). ***B***, All structures in a hand segmented synapse are separated with the same color code as A to show the general morphology of material in each compartment. ***C***, Examples structures from ***A*** segmented using the local thresholding method, demonstrating how the thresholding method affects morphology. ***D***, All local threshold segmented structures of the synapse separated by compartment, demonstrating the similarity in the amount of material connected through transmembrane structures by the two segmentation methods. Scale bars: 40 nm.

some intracellular structures were shared between transcleft structures, similar numbers of objects were found in all three compartments.

We adopt the term transsynaptic assemblies to refer to a transcleft structure and the collection of structures directly connected to it (Fig. 2*A*). Transsynaptic assemblies contact all synaptic vesicles with midpoints within 30 nm of the synaptic membrane, between six and eight vesicles. 22% (60 of 267) of assemblies directly contact synaptic vesicles. Between 7 and 14 of all synaptic vesicles directly contact assembly structures per excitatory synapse. Vesicles could contact as many as eight transsynaptic assemblies. The number of transsynaptic assemblies contacting a single vesicle did not correlate with distance to the synaptic membrane. We have not determined a pattern of assembly connectivity or composition that correlates with vesicle proximity to the active zone membrane.

The reported results are from hand segmented objects, but tomograms were also segmented using local thresholding, as an objective check on the hand segmented findings. In three excitatory clefts, hand segmentation yielded 267 structures spanning the cleft, with a combined volume of 8.6×10^4 nm^3. In contrast, local thresholding yielded 207 structures, with a comparable volume of 1.2×10^5 nm^3. Threshold structures often exhibited a bulkier appearance than hand segmented structures (Fig. 2*A*,*C*); this included some large cleft structures that would have been considered separate objects by hand segmentation. Thresholding also resulted in some incomplete structures because of saturated black levels. Even so, local thresholding corroborated the connectivity of components into transsynaptic assemblies. 64% (133 of 207) of thresholded transcleft structures connected to membrane-bound structures in both presynaptic and postsynaptic compartments, only 1% less than the proportion found by hand segmentation.

Transsynaptic assemblies are diverse

Assembly components possessed diverse morphologies. Each hand segmented structure was assigned a composite of morphology-based descriptions. Of 214 presynaptic components, 68 associated with synaptic vesicles. 28% (19 of 68) of these assembly components were described as short docking tethers (Fig. 3*B*,*D*) and 24% (16 of 68) as large cluster filament extensions (long filamentous extensions from the active zone with periodic extensions), as described in Cole et al. (2016; Fig. 3*F*). In addition, 12% (8 of 68) were described as bulky complexes abutting synaptic vesicles. This rectangular complex had dimensions: ~10 nm wide, 20 nm long, and 15 nm high (Fig. 3*E*). A more common and compact variation on this structure often had long extensions that contacted vesicles further from the membrane. We describe these as globular bases, and 25% (17 of 68) of synaptic vesicle-associated components had this type of base (Fig. 3*C*).

Assemblies included each transcleft elements described in High et al. (2015). Of the 267 observed synaptic transcleft structures, 30% were described as straight (Fig. 3*G*), 18% globular, 17% S shape (Fig. 3*I*,*L*), and 13% bent (Fig. 3*H*,*K*). In addition, 15% of structures bifurcated (Fig. 3*J*–*L*). Bifurcating structures split at various distances from the membrane and did not target presynaptic or postsynaptic compartments specifically. These bifurcated elements could be two closely neighboring transcleft filaments indistinguishable from a single structure, adhesion complexes with more than one binding pair, or transcleft structures with auxiliary molecular associations. In synaptic vesicle-associated assemblies, nonbifurcated straight and s-shaped cleft components were most common.

Of the 250 observed postsynaptic assembly components, 40% (100 of 250) were described as vertical structures. Of these, 35% (35 of 100) were specifically described as vertical filaments (Fig. 3*O*,*P*), while 65% (65 of 100) were vertical extensions off a base structure (Fig. 3*Q*,*R*). There were three typical base structures, flat bases (23 with vertical extensions, 33 without; Fig. 3*O*), taller globular bases (26 with, 29 without; Fig. 3*Q*), and far bulkier square bases (16 with; 6 without; Fig. 3*R*). Vertical filaments likely include vertical MAGUK scaffolding like PSD-95. These 10- to 25-nm-long filament structures extended at angles between 60° and 90° from the membrane and had an average volume of 480 nm^3. 70% (43 of 250) of structures were described as short horizontal filaments lying along the postsynaptic membrane (Fig. 3*N*), often with the transmembrane structure

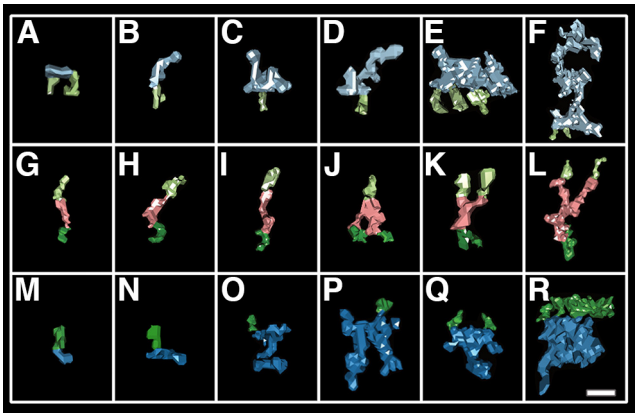

Figure 3. Samples of the diverse assembly components found in each compartment. A typical transsynaptic assembly has at least one intracellular component on each side of the synapse but may contain multiple. In this figure, a selection of six hand segmented assembly structures from each compartment are displayed in a grid ordered by volume. Each structure is shown with its transmembrane constituents (presynaptic, light green; postsynaptic, dark green). ***A–F***, Examples of membrane-bound presynaptic structures (light blue). ***G–L***, Examples of transcleft structures (pink) that constitute the core of an assembly. ***M–R***, Examples of postsynaptic membrane-bound structures (dark blue). Scale bar: ~10 nm.

contacting near the center of mass. These filaments were shorter than the vertical filaments with an average volume of 280 nm^3. Interestingly, within the globular base class were mound structures with centrally positioned vertical extensions like those associated with AMPA receptors proposed by Chen et al. (2008a; Fig. 3*Q*). The mounds were typically between 10 and 15 nm in diameter at the base and 15–20 nm high. Within the larger square class were large cuboid masses with an asymmetrically positioned vertical extension attached, resembling those Chen associated with NMDA receptors (Fig. 3*R*). Each postsynaptic base type was found in assemblies associated with synaptic vesicles, roughly 15 each, as were the horizontal filaments.

In both presynaptic and postsynaptic compartments, we found structures 2–6 nm in diameter extending up to 6 nm from the membrane (Fig. 3*A*,*M*). We called these small protrusions nubs. Nubs occasionally dot the parameter of synaptic vesicle clusters but are more often distributed outside of the synapse. Vesicle clusters are subpopulations of vesicles within the synapse's larger vesicle cloud. Typically, two or three are found near the active zone per synaptic tomogram. Within the synapse, nubs make up 20% (43 of 214) of presynaptic structures and 14% (34 of 250) of postsynaptic structures. Outside the synapse, nubs make up 38% (71 of 185) presynaptic structures and 31% (53 of 173) of postsynaptic structures, making it the most abundant structure outside the synapse. Based on their size and distribution, nubs could be intracellular extensions of transmembrane components of cell adhesion molecules. This could explain why nearly all transcleft structures have some intracellular connection.

In addition to morphology, we analyzed the volume of structures and found a stark difference in volume of structures inside and outside the synapse. Structure volume drops considerably at the edge of the synapse, marked by the farthest vesicles of the synapses' vesicle cloud along the active zone membrane. The average volume of structures in all compartments was 470 nm^3 inside the synapse but dropped to 210 nm^3 outside the synapse.

Transsynaptic assemblies classified by size and shape

The collection of components in an assembly appear to physically connect rather than merely align. Thus, an assembly with components on both sides of the synapse, a *full assembly*, could functionally coordinate components across the synapse. In all, 65% (173 of 267) of hand segmented excitatory assemblies fit this description, and three common types were found (Fig. 4). The first full assembly type, a *simple assembly*, contains small structures in each intracellular compartment with the sum of all intercellular structures not exceeding 1500 nm^3. Simple assembly components consisted of flat structures and vertical filaments intracellularly, and bifurcated or straight structures extracellularly. Of the full assemblies, 15% (41 of 267) were classified as simple type. Only 11 were in the synapse and only two contacted synaptic vesicles. In the synapse, this assembly type is distributed between synaptic vesicle clusters and in regions of low object-density in the postsynaptic density. 34% (14 of 41) of simple assemblies were a subpopulation we called *nub-only*, with only nub structures on both sides of the synapse.

A second assembly type, the *complex assembly*, contains at least one medium sized structure (larger than 600 nm^3) in both intracellular compartments; the combined volume of intracellular components exceeded 3000 nm^3 but could be as large as 8000 nm^3. Complex assemblies made up 12% (32 of 267) of all assemblies. Examples of structures found in complex assemblies include large cluster filament extensions and both the large and small rectangular complexes in the presynaptic compartment and all three bulky postsynaptic base structures. While each transcleft component type was found in complex assemblies, the S-shape and bent types were the most common. This assembly type groups near synaptic vesicle clusters and are often entangled through shared components. Of 32 complex assemblies, 20 contacted synaptic vesicles. No complex assemblies were found outside of the synapse.

The third assembly type, the *asymmetrical assembly*, has large intracellular structures in one compartment while the other side's components are 50% or smaller in volume, making them presynaptic or postsynaptic-heavy. Essentially, asymmetrical assemblies are a combination of simple and complex assembly types. Asymmetric assemblies made up 36% (97 of 267) of assemblies. Of the 97 asymmetrical assemblies, 56% were postsynaptic-heavy. A single nub opposing a large volume across the cleft was common in asymmetrical assemblies, especially in postsynaptic-heavy assemblies (16 of 38).

Asymmetrical assemblies were the assembly type most likely to contact synaptic vesicles, 24% (23 of 97) contacted a synaptic vesicle. This assembly type was found both inside and outside the synapse, however those with intracellular structure volume over 1400 nm^3 were only inside the synapse. The mean volume of asymmetric intracellular components combined was 1270 nm^3 inside and 630 nm^3 outside the synapse.

Transsynaptic assemblies cluster into domains of association

Intracellular components sometimes contacted more than one transsynaptic assembly, resulting in discernible domains of association. In these instances, two or more transcleft structures connected to the same intracellular object at distinctly different points with their respective transmembrane structures. We considered these assemblies linked and their intracellular components grouped. We referred to grouped intracellular components as *association domains*. Only 16% of presynaptic (34 of 214) and 24% of postsynaptic (61 of 250) synaptic intracellular structures were shared by two to four transcleft structures. However, 56% of presynaptic components (120 of 214) and 53% of postsynaptic components (132 of 250) were

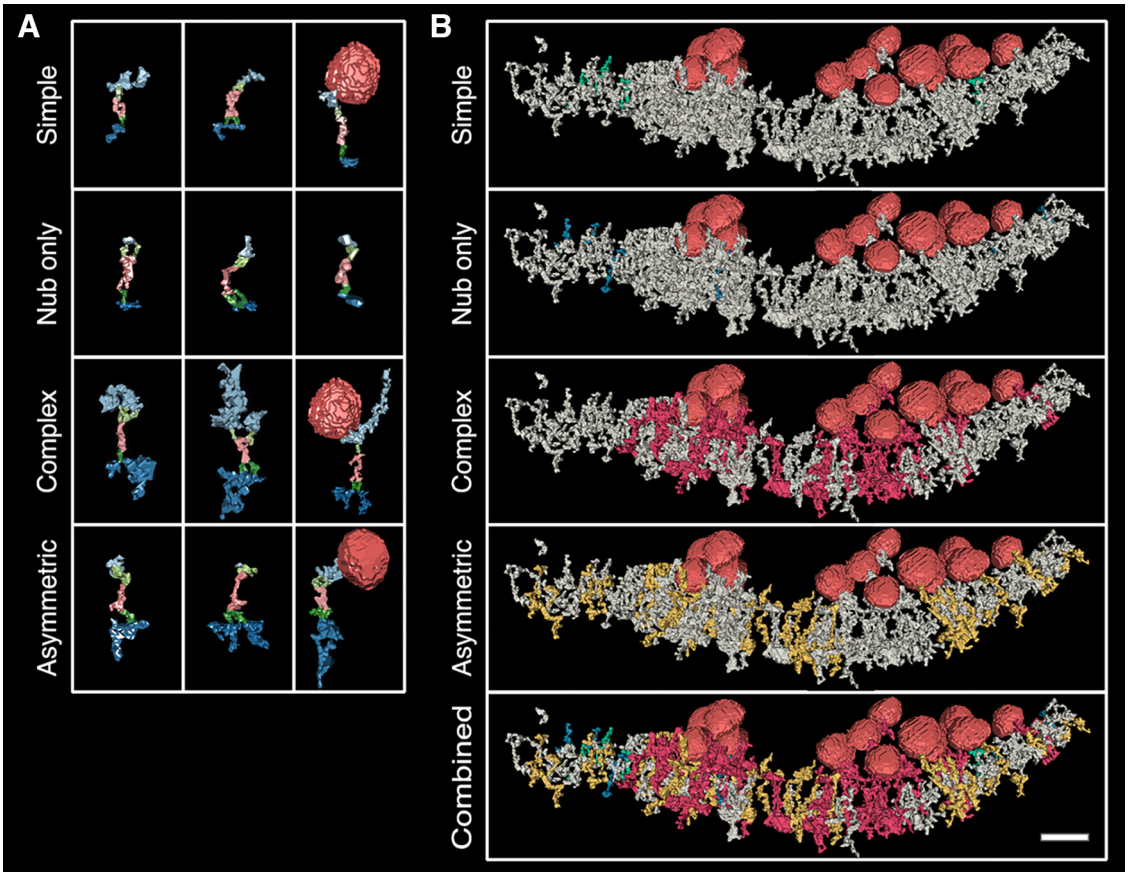

Figure 4. Transsynaptic assemblies can be classified by the number of components (complexity) or intracellular component volume. ***A***, Each row includes three different rendered examples of an assembly type, described in the text. Presynaptic intracellular and transmembrane structures are light blue and light green, respectively; transcleft structures are pink; and postsynaptic intracellular and transmembrane structures are dark blue and dark green, respectively. Synaptic vesicles are rendered in red. Some complex and asymmetric renderings exceeded the box height were scaled slightly to fit. ***B***, One assembly type is colored in each synapse rendering (simple are green; nub only are blue; complex are red; asymmetric are yellow), and all other structures are gray with the exception of vesicles, which are red. Scale bar: 40 nm.

grouped into an association domain. This was because of component sharing within their transsynaptic assemblies.

Because association domains stem from transsynaptic assemblies, an association domain in one compartment aligns across the cleft to a counterpart component or domain (Fig. 5*A*,*C*). We assume that some intracellular structures are collections of molecular complexes so close together they cannot be teased apart because of stain and resolution limits, especially large structures. Association domains linked 55% of assemblies (146 of 267) throughout synapses, but often occur around and include synaptic vesicles, forming synaptic vesicle centered associations (Fig. 5*C*, *D*). 27% of assemblies in association domains (40 of 146) directly associate with synaptic vesicles. The median number of assemblies per domain pair was four for hand segmented synapses and five for threshold. Last, assemblies could belong to more than one domain, as defined above.

Extrasynaptic areas and inhibitory synapses also include transsynaptic assemblies and association domains

As mentioned above, assemblies occurred outside the synapse. While smaller than assemblies within the synapse, full extrasynaptic assemblies were abundant (134 of 199). Half of all extrasynaptic assemblies form association domains (96 of 199); the median number of assemblies per domain pair is three for hand segmented synapses and two for threshold.

Two symmetrical synapses, classified as inhibitory, were analyzed. Both were completely segmented using local thresholding in parity to excitatory sets, but only partially hand segmented (Fig. 6). The mean volume of synaptic structures was larger (455 nm^3) than that of extrasynaptic structures (247 nm^3), showing a reduction of extrasynaptic structure volume similar to that in excitatory synapses (Fig. 6*D*,*E*). Of all transsynaptic assemblies in inhibitory synapses, 62% had both presynaptic and postsynaptic intracellular structures (42 of 68). Only 13% of postsynaptic (7 of 57) and 9% of presynaptic structures (nine of 68) associated with more than one transcleft filament.

Hand segmentation focused on the morphology of transcleft assemblies associated with synaptic vesicles. In the presynaptic compartment, short tethers (eight of 22) and flat bases with tethers (eight of 22) were commonly found contacting vesicles. Globular bases, square bases, and cluster filaments (2 each) were also present and contacted synaptic vesicles, as described in excitatory synapses. In the postsynaptic compartment, neither well defined mound structures nor scaffolding structures appeared in the inhibitory postsynaptic compartment. Instead, short ~15 nm angled extensions emerged from globular complexes (six of 20), ~900 nm^3 in diameter on the synaptic membrane. Last, nubs were found in both presynaptic and postsynaptic intracellular compartments.

Notably, 78% of transsynaptic assemblies (207 of 267) in excitatory synapses are not directly associated with synaptic vesicles,

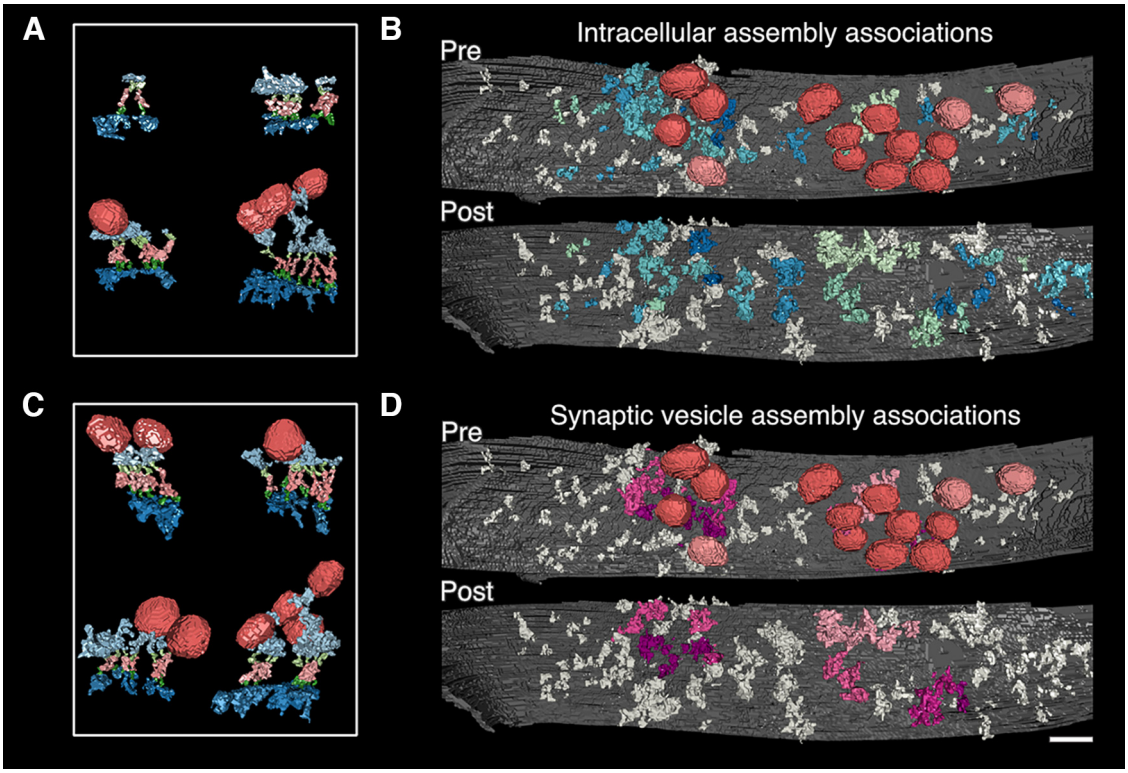

Figure 5. Shared intracellular components link transsynaptic assemblies and cause association domains of presynaptic and postsynaptic intracellular material that pair across the synapse. In many cases, an intracellular structure will connect more than one transcleft structure, linking the assemblies and their components. We call the resulting clusters of intracellular material "association domains." ***A***, In four examples of association domains, a single shared intracellular structure was selected, and all connected assemblies and structures were rendered, including synaptic vesicles (structure color code: presynaptic transmembrane and intracellular, light green and light blue; synaptic vesicles, red; postsynaptic transmembrane and intracellular, dark green and dark blue; transcleft, pink). ***B***, Each linked presynaptic and postsynaptic association domain is colored a single shade of blue or green. Synaptic vesicles are red if connected to a domain but otherwise pink. All other structures are gray. ***C***, In four examples, a single synaptic vesicle was selected, and all connected assemblies and structures are rendered to illustrate the clustering of material around synaptic vesicles through association domains. ***D***, Not all association domains associate with synaptic vesicles. Here, synaptic vesicle-associated domains are indicated by coloring linked presynaptic and postsynaptic structures in shades of pink. Other structures are colored gray. Again, synaptic vesicles-associated with domains are colored red and otherwise pink. In ***A*** and ***C***, renderings are oriented and scaled for comparison. Scale bar: 40 nm.

and 85% in inhibitory synapses (58 of 68; from threshold data). Clearly, transsynaptic assemblies do not exist entirely to align synaptic vesicles to postsynaptic receptors, but these other functions are yet to be determined.

Discussion

Our tomographic renderings demonstrate the ubiquitous connectivity of structures linking the three synaptic compartments. In excitatory synapses, 65% of all cleft-spanning structures link both presynaptic and postsynaptic intracellular complexes (Fig. 1*C*). We classify these as full transsynaptic assemblies, the recently-described assemblages of synaptic components aligning across the synaptic cleft (Martinez-Sanchez et al., 2021). The minimum number of cleft-spanning objects within an excitatory synapse was 64. Within that 64, 45 were the cleft component of full assemblies, which exceeds the estimated number of synaptic protein-nanodomain puncta or nanocolumns observed by super-resolution light microscopy (up to six; Tang et al., 2016; Biederer et al., 2017). We conclude that each assembly pairs specific sets of proteins across the cleft while also coalescing to bring key synaptic proteins together into a smaller number of functional nanocolumns.

Transsynaptic assemblies distribute based on size and complexity

The range of potential transsynaptic assemblies is vast, as cleft molecules like synaptic cell adhesion molecules have many binding partners. For example, consider the presynaptic cell adhesion molecule neurexin. Neurexin associates with synaptotagmin and Mint, and both associate with synaptic vesicles (O'Connor et al., 1993; Biederer and Südhof, 2000; Reissner et al., 2013). Neurexin's postsynaptic cell adhesion partners include LRRTMs and neuroligins (Südhof, 2017). Neuroligin binds PSD-95 (Irie et al., 1997), while LRRTMs wrangle AMPA receptors (Ramsey et al., 2021). PSD-95 interacts with AMPA receptors via stargazin (Schnell et al., 2002) and NMDA receptors directly (Kornau et al., 1995; Niethammer et al., 1996). Numerous other proteins could replace or adorn any component here (Togashi et al., 2009; Missler et al., 2012; Südhof, 2017; Liu, 2019).

Untangling these complexes and providing structural identities is limited by the available data, but we will discuss patterns. Notably, complex assemblies occur only at the synapse and typically in synaptic vesicle clusters, small clusters of vesicles near the active zone membrane (Fig. 4*B*, Complex). RIM and RIM-BP are candidates for the core presynaptic component in these assemblies because of their many binding partners and association with synaptic vesicle release (Südhof, 2012, 2018; Acuna et al., 2016). AMPARs and PSD-95 are candidates for postsynaptic components. These components align with RIM and RIM-BP (Tang et al., 2016) and knocking out RIM and RIM-BP partially inhibits that alignment (Acuna et al., 2016). Last, nearly all proximal synaptic vesicles connect to at least one of these assemblies directly or indirectly, in our renderings of excitatory synapses. Thus, some of these assemblies clearly belong to machinery for

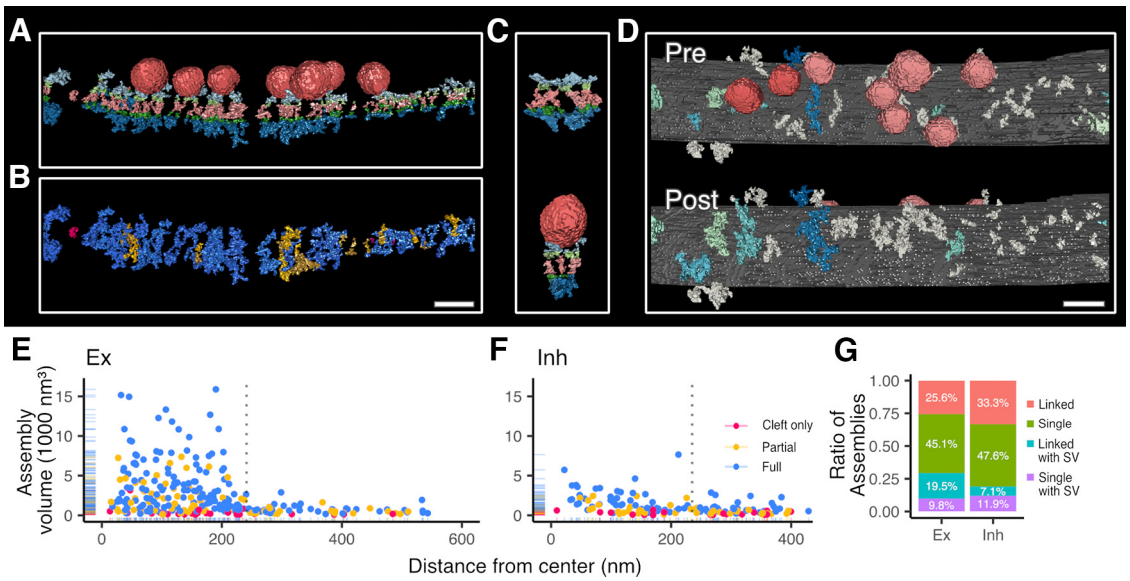

Figure 6. Inhibitory synapses have transsynaptic assemblies and association domains, although less dense and lower assembly-volume than excitatory synapses. ***A***, An inhibitory synapse is rendered with all transsynaptic assembly-associated synaptic vesicles and structures to indicate the abundance of structures on both sides of the synapse (structures are color coded: associated synaptic vesicles, red; presynaptic intracellular material and transmembrane material, light blue and light green respectively; postsynaptic intracellular material and transmembrane material, dark blue and dark green respectively; and cleft material, pink). ***B***, The same inhibitory synapse is instead color coded to indicate the distribution of full transsynaptic assemblies (assembly color code: full, blue; partial, yellow; and cleft only, red). ***C***, In two examples, a single intracellular structure was selected and all its connected assemblies with their structures are rendered including synaptic vesicles to depict association domains. ***D***, Association domains in an inhibitory synapse are indicated by assigning a blue or green shade to each cluster of linked transsynaptic assemblies and structures, otherwise structures are colored gray. Synaptic vesicles connecting to an association domain are colored red but pink if not. ***E***, ***F***, For thresholded excitatory (***E***) and inhibitory (***F***) synapses, the distribution of assembly volumes is visualized relative to the distance from the estimated center of the synapse. The center of the synapse is set as the halfway point, in the cleft, between the furthest synaptic vesicles associated with transsynaptic assemblies. The maximum synaptic vesicle distance is marked by a vertical dotted line. ***G***, The ratio of different types of transsynaptic assemblies in excitatory and inhibitory synapses (again, from thresholded data for comparison). The majority of transsynaptic assemblies are without synaptic vesicle association (linked assemblies are colored pink, and single assemblies in green) However, transsynaptic assemblies can contact vesicles directly (single with SV, colored purple) or through an association domain (linked with SV, colored blue). In ***A***, ***C***, renderings are oriented and scaled for comparison. ***A***, ***B***, ***D***, Scale bars: 40 nm.

the organization of neurotransmitter release and capture. However, the myriad complex assemblies that do not fit these descriptions warrant more study.

At the other end of the spectrum, the nub-only assembly has intracellular structures extending no more than 6 nm into the cell, a minimal intrusion. These are almost exclusively extrasynaptic, except for their presence between synaptic vesicle clusters (Fig. 4*B*, Nub only). Simple assemblies are more common in the synapse, but typically do not directly associate with synaptic vesicles. We suggest that simple assemblies, including nub-only, function as pure cell adhesion complexes.

The last and most abundant type are the asymmetric assemblies. These appear to be the base mode of pairing components across the cleft, given their relatively uniform distribution in and outside the synapse. Tang et al. (2016) indicates dramatic reorganization of aligned components after stimulation, which suggests that some asymmetrical assemblies could in fact be complex assemblies transitioning components, especially those located within the vesicle clusters and with direct association with vesicles.

More samples and computational structural comparison and differentiation will help to elucidate the functional significance of these three assembly types and identify additional types.

Assembly components connect into functional units

We assume that assembly components physically bind together, because our data shows transcleft, transmembrane, and intracellular structures that physically connect or overlap. Our data shows that 89% of transcleft structures connect to at least one intracellular compartment and 66% connect to both, suggesting a significant transsynaptic linkage. Transcleft structures are the foundation of assemblies and manifest as single, cleft-spanning structures which appear to lean (Fig. 3*G–L*). We expect that transcleft structures correspond to opposing pairs of complexed synaptic cell adhesion proteins which have consistent binding partners (Missler et al., 2012) and are often strong and persistent links between presynaptic bouton and postsynaptic density that can survive subcellular fractionation (Gray and Whittaker, 1962; Heynen et al., 2000; Holman et al., 2007; Fernández-Busnadiego et al., 2010). This suggests that transcleft structures can form a consistent anchoring spot for intracellular components.

The same transcleft filament could serve as an anchoring spot for any intracellular molecular complexes with compatible binding sites to organize around. In this way, the molecular composition of transsynaptic assemblies could be temporary or long-lasting, depending on binding or synaptic dynamics. In this model, the function of an assembly is primarily determined by the transcleft component.

Association domains and linked assemblies resemble nanodomains and nanocolumns

Our results show that assemblies share components, and this links assemblies. The collective intracellular components of a group of linked assemblies produces structural domains on both sides of the synapse (Fig. 5). We propose that association domains within a single compartment correspond to nanodomains, as described by Tang et al. (2016), and nanocolumns (aligned nanodomains across the cleft) are the association domains connected across the cleft by assemblies. Nanocolumns are typically associated with vesicle release machinery, and our

renderings show large association domains pairs are present within synaptic vesicle clusters (Fig. 5*D*).

Our renderings display the heterogeneity of nanodomains and nanocolumns. For instance, an association domain with short connections to one synaptic vesicle could also include a long cluster filament that links vesicles further in the vesicle cloud, linking them all to the active zone and possibly calcium channels, as previously reported (Figs. 4*A*, Complex, 5*C*; Wong et al., 2014; Cole et al., 2016). Also, many association domains were not associated with synaptic vesicles, so transsynaptic alignment could serve other functions beyond synaptic transmission.

Tomography with high-pressure freezing and freeze-substitution provides clarity in structure but cannot resolve the separation of structures less than a nanometer apart, so shared structures with a large footprint may represent closely bundled complexes rather than a single large complex.

Structural complexity is found mainly within the excitatory synapse

In our tomograms, simple and asymmetric assemblies populate the extrasynaptic region (Fig. 4*B*). The average volume of extrasynaptic intracellular structures is halved relative to inside the synapse (Fig. 6*E*), because assemblies with large intracellular structures are rare outside the synapse. This supports the idea that simple and nub-only assemblies are primarily cell adhesion molecules, as fewer large molecular complexes come together outside the synapse. We suggest that the simple assemblies between clusters of synaptic vesicles within the synapse perhaps mark channels of extrasynaptic-like domains within the synapse.

Bulky intracellular structures are lacking in inhibitory assemblies as well. Inhibitory assemblies are more spread out and are less likely to associate with synaptic vesicles. Also, association domains appear more asymmetrically distributed across the inhibitory synapse (Fig. 6), foreshadowed by our previous work (High et al., 2015).

Assemblies appear to be a common motif in connectivity between neurons. They appear in excitatory and inhibitory synapses, as well as extrasynaptic regions, and show differences that may help differentiate synapses and deduce identity of components with advanced analysis of many more synapses.

The eye is useful for descriptive analysis

Advanced automated segmentation methods yield remarkable renderings (Martinez-Sanchez et al., 2021; Peters et al., 2022), exceeding the local thresholding method in speed and clarity of morphology. Clearly, automated segmentation methods are the path forward for speed. That said, hand segmentation remains a useful method for descriptive analysis and model correction, because hand segmentation allows for close examination of structural context in raw micrographs. The power of electron microscopy is the combination of resolution and structural context. The eye and hand make great use of both.

Conclusion

In conclusion, biochemical analysis of the synapse clearly shows that synaptic cell adhesion molecules bind with transmembrane receptors and intracellular material. Here, our renderings visualize how that system of contiguous binding of molecules across the synapse manifests structurally and how that same system aligns clusters of material in separate cells. Our renderings, together with the cryo-electron tomography renderings of Martinez-Sanchez et al. (2021) and the super-resolution fluorescent tagging of Tang et al. (2016), convince us that these transsynaptic assemblies are involved in the alignment of synaptic vesicle release site material with postsynaptic receptors via transsynaptic assembly association domains. However, in our renderings, only 20% of excitatory full assemblies are associated with a synaptic vesicle (10% in inhibitory synapses; from threshold data), so transsynaptic assemblies are likely coordinating material for other synaptic functions, perhaps representing a two-way communication of molecular requirements outside the neurotransmitter system. These are early days in our understanding of how the synaptic compartments coordinate, and we are now faced with a variety of new possibilities of understanding the functions of the synapse.

References

Acuna C, Liu X, Südhof TC (2016) How to make an active zone: unexpected universal functional redundancy between RIMs and RIM-BPs. Neuron 91:792–807.

Bates AS, Manton JD, Jagannathan SR, Costa M, Schlegel P, Rohlfing T, Jefferis GSXE (2020) The natverse, a versatile toolbox for combining and analysing neuroanatomical data. Elife 9:e53350.

Biederer T, Südhof TC (2000) Mints as adaptors. J Biol Chem 275:39803–39806.

Biederer T, Kaeser PS, Blanpied TA (2017) Transcellular nanoalignment of synaptic function. Neuron 96:680–696.

Burette AC, Lesperance T, Crum J, Martone M, Volkmann N, Ellisman MH, Weinberg RJ (2012) Electron tomographic analysis of synaptic ultrastructure. J Comp Neurol 520:2697–2711.

Chen X, Winters C, Azzam R, Li X, Galbraith JA, Leapman RD, Reese TS (2008a) Organization of the core structure of the postsynaptic density. Proc Natl Acad Sci U S A 105:4453–4458.

Chen X, Winters CA, Reese TS (2008b) Life inside a thin section: tomography. J Neurosci 28:9321–9327.

Chen X, Nelson CD, Li X, Winters CA, Azzam R, Sousa AA, Leapman RD, Gainer H, Sheng M, Reese TS (2011) PSD-95 is required to sustain the molecular organization of the postsynaptic density. J Neurosci 31:6329–6338.

Chen X, Winters C, Azzam R, Sousa AA, Leapman RD, Reese TS (2014) Nanoscale imaging of protein molecules at the postsynaptic density. In: Nanoscale imaging of synapses: new concepts and opportunities (Nägerl V, Triller A, ed), pp 1–21. New York: Humana.

Chen X, Levy JM, Hou A, Winters C, Azzam R, Sousa AA, Leapman RD, Nicoll RA, Reese TS (2015) PSD-95 family MAGUKs are essential for anchoring AMPA and NMDA receptor complexes at the postsynaptic density. Proc Natl Acad Sci U S A 112:E6983–E6992.

Cole AA, Chen X, Reese TS (2016) A network of three types of filaments organizes synaptic vesicles for storage, mobilization, and docking. J Neurosci 36:3222–3230.

Fernández-Busnadiego R, Zuber B, Maurer UE, Cyrklaff M, Baumeister W, Lucic V (2010) Quantitative analysis of the native presynaptic cytomatrix by cryoelectron tomography. J Cell Biol 188:145–156.

Gray EG (1969) Electron microscopy of excitatory and inhibitory synapses: a brief review. Prog Brain Res 31:141–155.

Gray EG, Whittaker VP (1962) The isolation of nerve endings from brain: an electron-microscopic study of cell fragments derived by homogenization and centrifugation. J Anat 96:79–88.

Heynen AJ, Quinlan EM, Bae DC, Bear MF (2000) Bidirectional, activity-dependent regulation of glutamate receptors in the adult hippocampus in vivo. Neuron 28:527–536.

High B, Cole AA, Chen X, Reese TS (2015) Electron microscopic tomography reveals discrete transcleft elements at excitatory and inhibitory synapses. Front Synaptic Neurosci 7:9.

Hirokawa N, Sobue K, Kanda K, Harada A, Yorifuji H (1989) The cytoskeletal architecture of the presynaptic terminal and molecular structure of synapsin 1. J Cell Biol 108:111–126.

Holman D, Feligioni M, Henley JM (2007) Differential redistribution of native AMPA receptor complexes following LTD induction in acute hippocampal slices. Neuropharmacology 52:92–99.

Irie M, Hata Y, Takeuchi M, Ichtchenko K, Toyoda A, Hirao K, Takai Y, Rosahl TW, Südhof TC (1997) Binding of neuroligins to PSD-95. Science 277:1511–1515.

Kornau HC, Schenker LT, Kennedy MB, Seeburg PH (1995) Domain interaction between NMDA receptor subunits and the postsynaptic density protein PSD-95. Science 269:1737–1740.

Kremer JR, Mastronarde DN, McIntosh JR (1996) Computer visualization of three-dimensional image data using IMOD. J Struct Biol 116:71–76.

Landis DM, Hall AK, Weinstein LA, Reese TS (1988) The organization of cytoplasm at the presynaptic active zone of a central nervous system synapse. Neuron 1:201–209.

Linsalata AE, Chen X, Winters CA, Reese TS (2014) Electron tomography on γ-aminobutyric acid-ergic synapses reveals a discontinuous postsynaptic network of filaments. J Comp Neurol 522:921–936.

Liu H (2019) Synaptic organizers: synaptic adhesion-like molecules (SALMs). Curr Opin Struct Biol 54:59–67.

Martinez-Sanchez A, Laugks U, Kochovski Z, Papantoniou C, Zinzula L, Baumeister W, Lučić V (2021) Trans-synaptic assemblies link synaptic vesicles and neuroreceptors. Sci Adv 7:eabe6204.

Mayer ML, Vyklicky L (1989) The action of zinc on synaptic transmission and neuronal excitability in cultures of mouse hippocampus. J Physiol 415:351–365.

Missler M, Südhof TC, Biederer T (2012) Synaptic cell adhesion. Cold Spring Harb Perspect Biol 4:a005694.

Murdoch D, Adler D (2022) rgl: 3D visualization using OpenGL. Available at: https://github.com/dmurdoch/rgl and https://dmurdoch.github.io/rgl/.

Niethammer M, Kim E, Sheng M (1996) Interaction between the C terminus of NMDA receptor subunits and multiple members of the PSD-95 family of membrane-associated guanylate kinases. J Neurosci 16:2157–2163.

O'Connor VM, Shamotienko O, Grishin E, Betz H (1993) On the structure of the 'synaptosecretosome'. Evidence for a neurexin/synaptotagmin/syntaxin/Ca2+ channel complex. FEBS Lett 326:255–260.

Peters JJ, Leitz J, Guo Q, Beck F, Baumeister W, Brunger AT (2022) A feature-guided, focused 3D signal permutation method for subtomogram averaging. J Struct Biol 214:107851.

Ramsey AM, Tang AH, LeGates TA, Gou XZ, Carbone BE, Thompson SM, Biederer T, Blanpied TA (2021) Subsynaptic positioning of AMPARs by LRRTM2 controls synaptic strength. Sci Adv 7:eabf3126.

Reissner C, Runkel F, Missler M (2013) Neurexins. Genome Biol 14:213.

Schnell E, Sizemore M, Karimzadegan S, Chen L, Bredt DS, Nicoll RA (2002) Direct interactions between PSD-95 and stargazin control synaptic AMPA receptor number. Proc Natl Acad Sci U S A 99:13902–13907.

Siksou L, Triller A, Marty S (2009) An emerging view of presynaptic structure from electron microscopic studies. J Neurochem 108:1336–1342.

Südhof TC (2012) The presynaptic active zone. Neuron 75:11–25.

Südhof TC (2017) Synaptic neurexin complexes: a molecular code for the logic of neural circuits. Cell 171:745–769.

Südhof TC (2018) Towards an understanding of synapse formation. Neuron 100:276–293.

Szule JA, Harlow ML, Jung JH, De-Miguel FF, Marshall RM, McMahan UJ (2012) Regulation of synaptic vesicle docking by different classes of macromolecules in active zone material. PLoS One 7:e33333.

Tang AH, Chen H, Li TP, Metzbower SR, MacGillavry HD, Blanpied TA (2016) A trans-synaptic nanocolumn aligns neurotransmitter release to receptors. Nature 536:210–214.

Togashi H, Sakisaka T, Takai Y (2009) Cell adhesion molecules in the central nervous system. Cell Adh Migr 3:29–35.

Watanabe S, Rost BR, Camacho-Pérez M, Davis MW, Söhl-Kielczynski B, Rosenmund C, Jorgensen EM (2013) Ultrafast endocytosis at mouse hippocampal synapses. Nature 504:242–247.

Wong FK, Nath AR, Chen RH, Gardezi SR, Li Q, Stanley EF (2014) Synaptic vesicle tethering and the CaV2.2 distal C-terminal. Front Cell Neurosci 8:71.

Wickham H, et al. (2019) Welcome to the tidyverse. J Open Source Softw 4:1686.